

VISER: Visually-Informed System for Enhanced Robustness in Open-Set Iris Presentation Attack Detection

Byron Dowling Eleanor Frederick Jacob Piland Adam Czajka

{bdowlin2, efreder3, jpiland, aczajka}@nd.edu

University of Notre Dame

Notre Dame, IN, USA

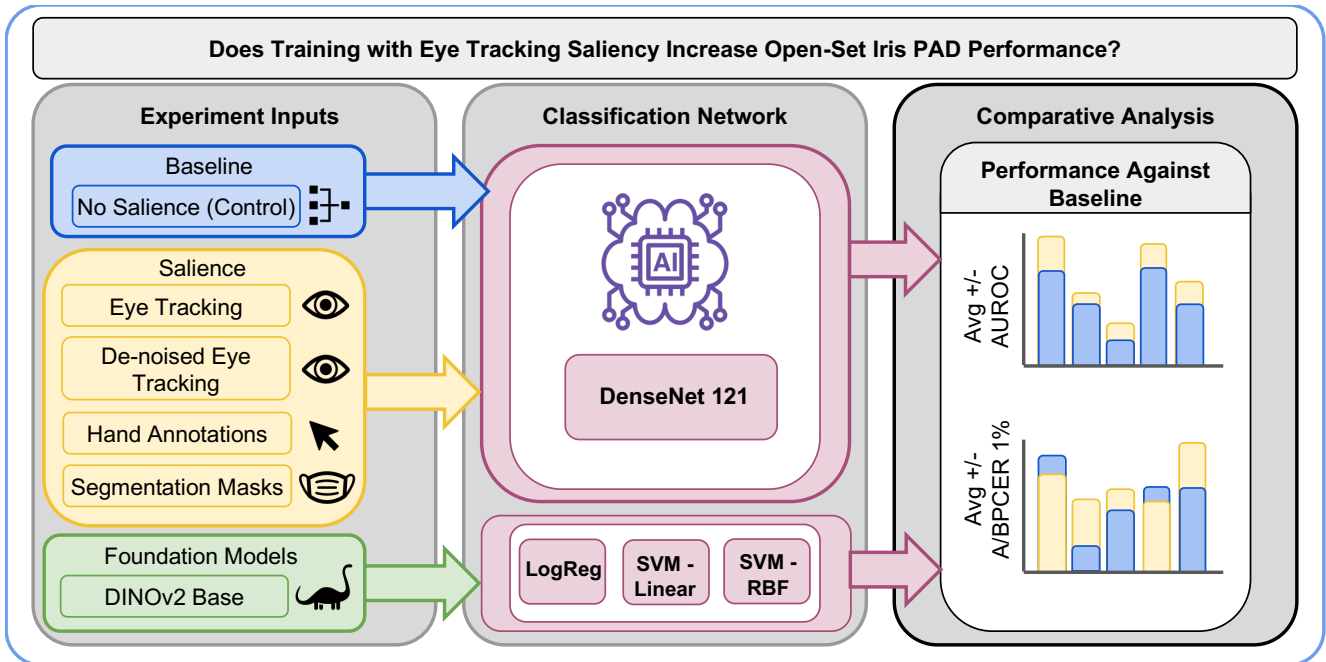


Figure 1. Experimental pipeline and contributions. A deep learning iris presentation attack detection model trained without saliency guidance serves as the baseline. We evaluate multiple saliency modalities through saliency-guided training, and further assess foundation model-sourced embeddings using logistic regression, linear-SVM, and RBF-SVM classifiers. Performance is reported in terms of Area Under the ROC curve (AUROC) and Attack Presentation Classification Rate (APCER) at 1% Bonafide Presentation Classification Rate (BPCER), expressed as relative improvement over the baseline trained traditionally.

Abstract

Human perceptual priors have shown promise in saliency-guided deep learning training, particularly in the domain of iris presentation attack detection (PAD). Common saliency approaches include hand annotations obtained via mouse clicks and eye gaze heatmaps derived from eye tracking data. However, the most effective form of human saliency for open-set iris PAD remains underexplored. In this paper, we conduct a series of experiments comparing hand annotations, eye tracking heatmaps, segmentation masks, and DINOv2 embeddings to a state-of-the-art deep learning-based

baseline on the task of open-set iris PAD. Results for open-set PAD in a leave-one-attack-type out paradigm indicate that denoised eye tracking heatmaps show the best generalization improvement over cross entropy in terms of Area Under the ROC curve (AUROC) and Attack Presentation Classification Error Rate (APCER) at Bona Fide Presentation Classification Error Rate (BPCER) of 1%. Along with this paper, we offer trained models, code, and saliency maps for reproducibility and to facilitate follow-up research efforts.

1. Introduction

Artificial Intelligence (AI) systems continue to play an increasingly pivotal role in every day tasks, and researchers and companies alike understand that a lack of trust in an AI model or a lack of trust in a model’s validity is a barrier to wide-scale adoption, particularly in critical tasks [22]. Among the core principles of Trustworthy AI is the idea of robustness, which means that good models should generalize well to unseen data classes and operate well in an open-set manner [22, 33, 37]. One popular technique for increasing a model’s ability to generalize to unknown attack types is utilizing human saliency (a map of features supporting the decision of a human examiner).

The use of human saliency in saliency-guided deep learning has seen increased interest in domains like synthetic face detection, x-ray abnormality detection, and iris PAD. The use of human saliency is used to improve the quality of model’s feature maps [14], and to directly guide the learning process of the model [7]. These techniques have shown to increase a model’s ability to generalize to unseen data types leading to more trustworthy and accurate performance. However collecting human saliency can be an expensive and time-consuming. While attempts to maximize the amount of saliency samples needed for the effective training of models has been explored [11, 12], there is still the question of what *form* of human saliency is optimal for the best transfer of expert’s knowledge into deep learning.

This paper focuses on the latter point as we present VISER, a Visually Informed System for Enhanced Robustness in open-set iris PAD. VISER attempts to address the trade-off between the continuous but noisy signal that eye tracking provides and the information loss that occurs in translation from visual to motor saliency. Results show that eye tracking heatmaps improve over the D-NetPAD cross entropy baseline for average AUROC and APCER at BPCER of 1% with denoised eye tracking showing the best performance of the variants. The **main contributions of this paper** are as follows:

- experiments evaluating open-set iris PAD models trained on different types of human saliency,
- a comparison of human saliency-guided models vs foundation models in open-set iris PAD,
- a method of denoising raw eye tracking gaze maps for the purposes of saliency-guided training leading to a state-of-the-art open-set iris PAD performance.

This paper is organized around the following research questions:

RQ1: Does the use of eye tracking saliency in saliency-guided training generalize better to unseen data than other saliency types?

RQ2: Does saliency-guided training outperform modern

PAD solutions utilizing foundational models in open-set iris PAD?

RQ3: Does de-noising eye tracking gaze maps improve over standard eye tracking gaze maps in saliency-guided training?

To facilitate follow-up research efforts, we offer the source codes, model weights, and saliency maps along with this paper for reproducibility purposes¹.

2. Related Work

2.1. Detection of Biometric Presentation Attacks

Iris recognition, widely regarded as a highly secure biometric modality, remains deployed in critical applications including border control, and personal identification [4, 13, 16]. Recent developments highlight financial authentication systems as an emerging application for iris biometrics, illustrating its expanding role for secure payments [44]. As with any security-critical system, iris recognition remains vulnerable to adversarial attempts that seek to compromise its integrity [13].

These attacks, known as presentation attacks, aim to manipulate a biometric system into an incorrect decision in one of two forms: identity concealment, where a malicious actor wishes to evade detection, or impersonation, where an actor attempts to obtain a false positive match [6, 13]. Iris presentation attacks include synthetic iris imagery generated using Generative Adversarial Networks (GANs) [31, 32, 55], as well as physical presentation attacks involving direct sensor interaction, such as post-mortem cadaver samples, high-resolution iris printouts, and artificial eyes [13, 58]. To combat these attacks, advances in deep learning have driven significant improvements in PAD systems [7, 11, 41]. More recent work has explored leveraging the general vision capabilities of image foundation models [51, 52] and designed novel loss functions to enhance multimodal alignment [65].

2.2. Human Saliency-Guided Training

Machine learning techniques have been shown to exceed human performance in the context of biometrics tasks [43]. However, alongside improving performance, there is growing demand for explainability which can be addressed by comparing model behavior to human experts [47]. Previous work has seen human salience used in tasks beyond Iris PAD: attention mechanisms [38], natural language processing [64], scene description [23, 27], handwriting, [21], and in the biometric task of synthetic face detection where machine saliency has been shown to compliment human expertise [7, 40, 45, 59]. Despite this broad adoption, to the best of our knowledge, no prior work has directly compared human derived saliency (*e.g.*, hand annotations and

¹<http://github.com/...> (redacted for anonymity)

eye-tracking data) and non-human saliency (*e.g.*, segmentation maps) for Iris PAD.

2.3. Visual vs Motor Saliency

Human saliency can be collected in a variety of forms, with hand annotations captured via mouse clicks and eye tracking from commercial eye tracking devices being two of the most prominent examples. Despite their popularity, these approaches differ substantially from a cognitive perspective in terms of cognitive load and the processing of information and visual stimuli [24, 30]. The distinction between the two saliency types is deeply rooted in the hierarchy of cognitive processing.

Eye gaze measured via eye tracking is a first-order physiological signal, whereas hand annotations (*e.g.*, mouse clicks or bounding boxes) are a second-order manifestation of conscious intent. In other words, eye tracking illustrates the direct link between what the eye fixates on and what the brain reflexively processes. Conversely, hand annotations exist primarily within the top-down task-driven attention space, indicating that visual stimuli are subject to a motor-planning bottleneck. That is, the brain must translate a visual perception into a physical movement, which tends to reflect a low recall for exploration [26].

The differences in granularity between the two saliency modalities are also evident from a spatial-temporal perspective. As a continuous stream of data, eye tracking can be susceptible to noise (*e.g.*, saccade movements, jitter, or distraction), whereas hand annotations represent a discrete and comparatively cleaner final result [15]. Beyond these differences, the type of saliency can influence the training of deep learning models. While mouse-contingent paradigms have been proposed as a scalable and cost-friendly substitute for eye tracking [29], prior work suggests that hand-based annotations often fail to capture the same spatial distributions as fixations [53]. These findings suggest that models trained on hand annotations may become over-reliant on high-level semantic features while ignoring the subtle, low-level visual cues captured by eye tracking. Although the differences between these two saliency modalities have been explored to some extent, their specific impact on iris PAD remains underexplored.

3. Experimental Design

To address our research questions, we perform several experiments testing different saliency methods under the same conditions. To test open-set robustness, we train each configuration in a leave-one-attack-type out manner and perform 12 independent runs per attack type with a total of 7 attack types tested. We first conduct a baseline measurement of iris PAD classification on the DenseNet121-based D-NetPAD architecture [25, 50] using standard cross-entropy loss, from here this configuration is simply referred

to as "XENT".

Next we test a variety of saliency sources in a saliency-guided training paradigm outlined in Boyd *et al.* [7] by utilizing the same DenseNet121 architecture with only the saliency source varying across the different configurations. Namely, each model is trained with a loss function that consists of cross-entropy and a saliency component. This saliency component uses the mean squared error of the model saliency with the target saliency in order to bring the model saliency in line with the desired outcome. Model saliency in our case means the model Class Activation Map (CAM) for a given sample.

Finally, with the emergence of capable foundation models in biometric tasks, we test three configurations using DINOv2-Base embeddings [42]. The details of these remaining configurations are outlined in the following sections.

3.1. Metrics

In accordance with ISO/IEC 30107 we report the Attack Presentation Classification Error Rate (APCER) at Bona Fide Presentation Classification Error Rate (BPCER) threshold of 1% for each configuration respectively [28], we also report the average Area Under the Receiver Operator Characteristic (AUROC) curve to provide easy comparison to other Iris PAD works. As we are comparing to the XENT baseline in all cases, specifically for a given model training method we report the difference between its performance and the XENT baseline performance. This does not change that a *lower* value is better for the APCER metric and a *higher* value is better the AUROC metric.

Our final ranking values are averages over all attack types compiled from multiple random variables: the variable for multiple runs per attack type left out, and the average over each category. Due to this we simply report point value ranking and exclude standard deviations. We define a better performance as lower (in the case of APCER) or higher (in the case of AUROC) ranking.

3.2. Dataset Sources

The images in our dataset reflect the following attack types and anomalies along with the bona fide samples and their sources: real irises [2, 3, 20, 34, 36, 48, 57, 62, 63], irises with textured contact lenses [34, 36, 62, 63], artificial (plastic eyes and glass prosthesis) eyes [36], diseased/unhealthy eyes [56, 57], printouts [20, 35, 36], synthetically-generated iris images [61], printouts of irises with textured contact lenses [36], and post-mortem iris images [60].

The eye tracking heatmaps were sourced from an eye tracking study conducted by Dowling *et al.* [17] who captured eye gaze heatmaps from a mixture of expert and non-expert examiners. Acquiring this variety of saliency allows us to perform the first study we are aware of comparing the

performance of different human saliency types for saliency guided training in the task of iris PAD.

3.3. Saliency Methods

3.3.1. Segmentation Masks

The segmentation masks used in the experiment were generated using a combination of open-source academic iris recognition methods [1]. As stated above, these segmentation masks were used as a part of a loss function to train a model instantiated from DenseNet-121, the full loss function consisting of cross-entropy and an MSE comparison of the model CAM saliency and the segmentation map for a given sample. We refer to this method as the *baseline saliency-based* method as segmentation maps represent the least intricate saliency.

3.3.2. Hand Annotations

The human hand annotation saliency we use was published in a human annotation study conducted by Boyd *et al.* [5]. Multiple individuals per sample were tasked with digitally annotating the important features on the sample. The final heat maps were generated by calculating the per-pixel average number of annotations for a sample, *i.e.* if a pixel was annotated by all individuals who annotated the sample, then the pixel would have a value of 1 and if annotated by no individuals, a value of 0.

We observed that the hand annotations typically have a lower CAM entropy than the eye tracking maps. As CAM entropy can affect model performance [45], we create multiple hand annotation methods at different entropies using gaussian blur. Blurring with a kernel of size 10 results in higher entropy on average than the eye tracking data and we refer to training done with these annotations as the *High Entropy* method. Blurring with a kernel of size 5 results in a matching entropy and we refer to training done with these annotations as the *Equal Entropy* method. Using the original annotations with no blur results in a lower entropy than the eye tracking saliency and we refer to training done with these annotations as the *Low Entropy* method.

3.3.3. Eye Tracking

Raw eye-tracking data collected from both expert and non-expert participants during iris image evaluations was processed into individual saliency heatmaps. For each participant normalized fixation coordinates were first corrected using per-participant polynomial remapping coefficients to account for calibration offset, and a Gaussian blur was applied to produce a continuous heatmap representation of visual attention. To produce a unified ground truth saliency map for each iris image, individual participant heatmaps were aggregated via a pixel-wise mean across all evaluators, expert and non-expert.

This pre-processing pipeline was applied for two saliency methods. The first we refer to as *Full Eye Tracking*,

as it uses captured attention across the full evaluation window. The second we refer to as *Initial Eye Tracking*, which captured visual attention during a participant’s first impression of the iris image. The motivation for examining both phases is to assess whether different visual features are prioritized when forming an initial judgment versus an overall assessment, and to determine which produces saliency maps better suited for saliency-guided training.

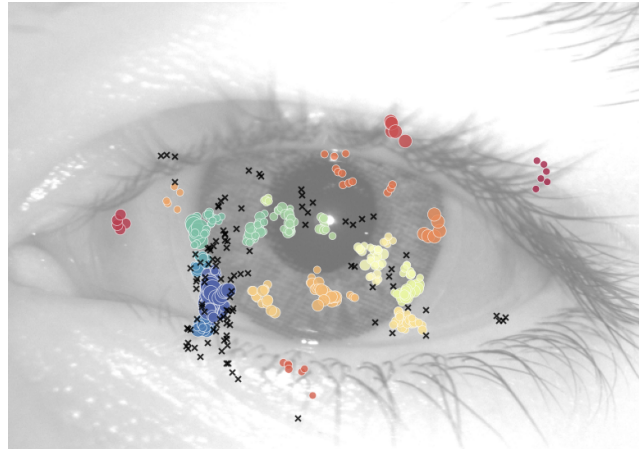


Figure 2. Example of applying HDBSCAN to de-noise the eye tracking data. Clusters made up of valid fixations are distinguished by color and larger marks denote longer fixations, not fixation area. Black crosses indicate fixations marked as noise excluded from the final saliency map.

However, eye tracking is a continuous stream of gaze points with many commercial models sampling at or above 200 Hz. While high sampling rates of these devices ensure maximum visual features are recorded, these devices are susceptible to noise due to involuntary eye movements such as micro-saccades and eye tremors [39, 46]. A common technique to reduce noise in eye tracking data, particularly for use in automatic area of interest (AOI) processing, is to apply a clustering algorithm to the fixation data to reduce outlier fixations that do not belong to a cluster according to a minimum cluster size such as DBSCAN or HDBSCAN [8, 18, 19, 54].

We define two more eye tracking methods using HDBSCAN to de-noise our eye tracking heatmaps. Specifically we apply HDBSCAN with a minimum cluster size of 5 and minimal sample count of 3 to each heatmap (See Fig. 2). We refer to training with the de-noised Full Eye Tracking saliency as the *De-noised Full ET* method and training with the de-noised Initial Eye Tracking heatmaps as the *De-noised Initial ET* method.

3.4. No Saliency: Foundation Model Baseline

Research has shown that foundation models show remarkable ability to distinguish both full-size and cropped iris

samples in closed-set presentation attack detection settings [51, 52]. Specifically, Redwan *et al.* used a variety of foundation models to obtain feature embeddings for iris PAD images and trained three standard classifiers, logistic regression (LogReg) [10], support vector machine (SVM)[9], and support vector machine with radial basis function kernel (SVM-RBF) [49] on the extracted features. In the task of iris PAD for full size irises, [42] suggests that the clear winner was DINOv2-Base. In accordance with these findings we test open-set iris PAD using the same methodology laid out by Redwan *et al.* resulting in our final three methods, *DINOv2+LogReg*, *DINOv2+SVM-Linear*, and *DINOv2+SVM-RBF*.

4. Results

4.1. Answering RQ1: Does the use of eye tracking saliency in saliency-guided training generalize better to unseen data than other saliency types?

We trained 12 independent models per attack-type-left-out for a total of 84 models for each method tested. For each run of 12 models, we report the average AUROC and APCER at BPCER 1% threshold. Table 1 shows these results expressed as each method’s improvement above the D-NetPAD XENT baseline where each row refers to a method and each column refers to the attack type that was left out during training with a final delta column summarizing the overall performance. Our findings indicate that initial phase eye tracking maps de-noised with HDBSCAN show the largest AUROC improvement over the XENT baseline at **0.061**. Entire and initial phase eye tracking maps also showed improved AUROC performance over XENT with improvements of **0.056** and **0.052** respectively. The remaining saliency-based methods either failed to surpass the XENT baseline entirely or improved it by only 0.01. **Thus the answer to RQ1 is affirmative, eye tracking saliency, particularly De-noised Initial Eye Tracking saliency, surpasses other saliency-based methods in open-set iris PAD.**

4.2. Answering RQ2: Does saliency-guided training outperform modern PAD solutions utilizing foundational models in open-set iris PAD?

When comparing the results of foundation models against XENT, the results are mixed. While DINOv2 + SVM-RBF showed improvement over XENT with an average AUROC of 0.048, both DINOv2 + LogReg and DINOv2 + SVM-Linear failed to improve the baseline. Similar to table 1, table 2 shows the same methods and their improvements above the D-NetPAD XENT baseline of APCER at BPCER at 1% for each attack type left out and a final delta column summarizing the overall performance. When comparing the

results of foundation models in this table, the results are poor. DINOv2 + LogReg was near even with XENT with an improvement of 0.0087 while DINOv2 + SVM-Linear and DINOv2 + SVM-RBF failed to improve the baseline. For the saliency-based methods, eye tracking methods showed better AUROC performance than segmentation masks and hand annotations as outlined in the previous section. When comparing the APCER at BPCER of 1%, Segmentation Masks and Hand Annotations fail to improve over the baseline. Eye tracking methods however show strong improvement over XENT with De-noised Initial ET improving by **0.1063** and Full Eye Tracking, De-noised Full ET, and Initial Eye Tracking improving by **0.0888**, **0.0857**, and **0.0852** respectively. With eye tracking methods improving XENT APCER by 0.08 or greater and only DINOv2 + LogReg improving the baseline at all, the answer to **RQ2** is clear, **saliency-guided training using eye tracking heatmaps outperform foundation models in open-set iris PAD.**

4.3. Answering RQ3: Does de-noising eye tracking gaze maps improve over standard eye tracking gaze maps in saliency-guided training?

The results of **RQ1** and **RQ2** indicate that eye tracking improved the XENT baseline in AUROC and APCER at BPCER 1%, but how do the de-noised methods compare against the standard eye tracking maps? Overall, De-noised Initial ET was the best performing method above XENT baseline in both AUROC and APCER at BPCER 1%. For AUROC, De-noised Initial ET reported an improvement of **0.0608** compared to Initial Eye Tracking at **0.0518** while in APCER at BPCER 1%, De-noised Initial ET showed an improvement of **0.1063** compared to Initial Eye Tracking’s **0.0822**. While the results show a clear advantage for de-noising the Initial Eye Tracking saliency maps, this is not the case for Full Eye Tracking maps. In both metrics, Full Eye Tracking outperforms De-noised Full ET with AUROC of 0.0562 > 0.0429 and APCER at BPCER 1% of 0.0888 > 0.0857 respectively. Therefore the answer to **RQ3** is mixed, **de-noising eye tracking gaze improves performance for Initial Eye Tracking saliency maps but is less effective on Full Eye Tracking saliency maps.**

4.4. Observations

To further contextualize our results, we report on observations from our experiments that may help inform state-of-the-art iris PAD model design. For example, AUROC results in Table 1 show that the D-NetPAD with cross entropy baseline performs quite well on the “contacts + print” attack type to the point that no other salience-based methods are able to improve upon its already superior performance. This high performance is somewhat explained by the similarity of the “printout” and “contacts + print” attack types being very similar. On the other hand, the “arti-

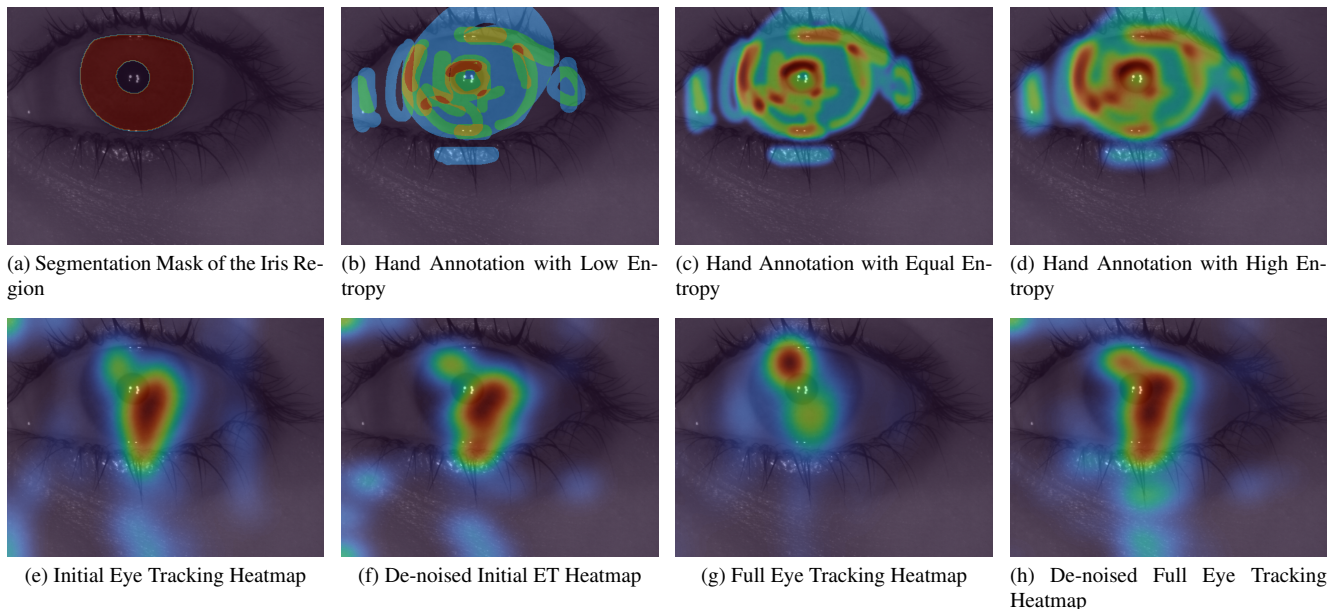


Figure 3. Sample saliency types captured for the same iris image.

Table 1. Compact AUROC Results (\uparrow). We report the absolute AUROC for the DenseNet (XENT) baseline, while all other rows show the change (Δ) relative to this baseline. Best results per column are bolded. Each column presents the results obtained for detecting this particular attack type, which was left out during training to guarantee an open-set iris PAD evaluation.

Method	Printout	Diseased	Post Mortem	Synthetic	Contacts + Print	Textured Contact	Artificial	Avg. Δ^*
Baseline Performance								
DenseNet (XENT)	<i>0.9169</i>	<i>0.6537</i>	<i>0.8012</i>	<i>0.6541</i>	<i>0.9717</i>	<i>0.7450</i>	<i>0.6550</i>	<i>0.7711</i>
Segmentation Masks								
Baseline Saliency-based	+0.0087	-0.0052	+0.0385	-0.0511	-0.0212	+0.0345	+0.0232	+0.0039
Hand Annotations								
High Entropy	-0.0184	+0.0520	+0.0073	-0.0712	-0.0123	-0.0050	+0.0175	-0.0043
Equal Entropy	-0.0010	+0.0847	-0.0098	-0.0122	-0.0021	+0.0274	+0.0277	+0.0164
Low Entropy	-0.0001	-0.0077	+0.0294	-0.0160	-0.0384	+0.0140	-0.0157	-0.0049
Eye Tracking Saliency								
Full Eye Tracking	+0.0473	+0.0282	-0.0468	+0.0941	-0.0155	+0.0474	+0.2387	+0.0562
Initial Eye Tracking	+0.0513	+0.0192	-0.0155	+0.0236	-0.0481	+0.0650	+0.2672	+0.0518
De-noised Full ET	+0.0604	+0.0345	-0.0820	+0.0621	-0.0782	+0.0597	+0.2438	+0.0429
De-noised Initial ET	+0.0627	+0.0574	-0.0645	+0.1090	-0.0453	+0.0372	+0.2692	+0.0608
Foundation Model (No Saliency)								
DINOv2 + LogReg	-0.0326	-0.1079	+0.0378	-0.0340	+0.0086	-0.0327	+0.1520	-0.0013
DINOv2 + SVM-Linear	-0.0523	-0.1247	-0.0033	-0.0613	+0.0017	-0.0351	+0.1737	-0.0145
DINOv2 + SVM-RBF	-0.0104	+0.0023	+0.1796	+0.1121	-0.0159	-0.0448	+0.1167	+0.0485

* Average is calculated across all attack types. Baseline row shows absolute AUROC.

Table 2. Same as in Table 1, except that compact Δ APCER @ BPCER=1% vs XENT Baseline (\downarrow) results are presented.

Method	Printout	Diseased	Post Mortem	Synthetic	Contacts + Print	Textured Contact	Artificial	Average Δ^*
Baseline Performance								
DenseNet (XENT)	0.5540	0.9377	0.8321	0.9831	0.2337	0.9167	0.9868	0.7777
Segmentation Masks								
Baseline Saliency-based	-0.0522	+0.0211	+0.0615	+0.0094	+0.0920	-0.0587	+0.0088	+0.0117
Hand Annotations								
High Entropy	+0.0257	+0.0088	+0.0166	+0.0169	+0.0623	-0.0294	+0.0000	+0.0144
Equal Entropy	+0.0879	-0.0535	+0.0423	+0.0094	+0.0173	-0.0341	+0.0088	+0.0112
Low Entropy	-0.0403	+0.0079	+0.0282	+0.0094	+0.1676	-0.0082	+0.0103	+0.0250
Eye Tracking Saliency								
Full Eye Tracking	-0.2765	-0.0210	+0.0153	-0.0664	+0.0824	-0.1198	-0.2353	-0.0888
Initial Eye Tracking	-0.2701	-0.0473	+0.0743	-0.0430	+0.1753	-0.0834	-0.3815	-0.0822
De-noised Full ET	-0.2893	-0.0412	+0.0717	-0.0927	+0.2194	-0.1127	-0.3552	-0.0857
De-noised Initial ET	-0.3617	-0.0412	+0.0551	-0.1413	+0.1600	-0.0599	-0.3552	-0.1063
Foundation Model (No Saliency)								
DINOv2 + LogReg	+0.1026	+0.0255	-0.1449	-0.0187	+0.0297	-0.0200	-0.0350	-0.0087
DINOv2 + SVM-Linear	+0.1914	+0.0219	-0.0924	-0.0037	+0.1408	+0.0035	-0.0935	+0.0240
DINOv2 + SVM-RBF	+0.2885	+0.0588	-0.5180	+0.0047	+0.2835	-0.0118	+0.0132	+0.0170

*We use point error estimator in this column (*i.e.*, without calculating and reporting standard deviations) only for ranking the methods, as the average is compiled from random variables of different distributions.

ficial” class shows the most room for improvement as every method but Low Entropy hand annotations surpassed the baseline with all forms of eye tracking showing large performance increases and De-noised Initial ET showing the single largest improvement across the board. Eye tracking methods as a whole showed broad improvement in the categories of ”printout” and ”synthetic” indicating that human feature selection in these categories is making a noticeable improvement.

In Table 2 we see similar trends as that of the AUROC table. None of the methods were able to improve APCER at BPCER 1% performance on the ”contacts + print” attack type as the XENT baseline is already a high performer. Eye tracking methods made large improvements with the best performing method in 4 of the 7 attack types belonging to an eye tracking saliency configuration. In particular, De-noised Initial ET made a 0.3617 improvement over baseline in the ”printout” category and Initial Eye Tracking made a 0.3815 improvement in the ”artificial” category indicating that even at permissive thresholds, these methods are able to reject a higher amount of attack samples than XENT.

While eye tracking saliency performed well across the board, hand annotations did not perform nearly as well. We

observe that this aligns with the literature in section 2.3 discussing the motor-planning bottleneck. In Boyd’s work [6], participant’s were instructed to highlight 5 regions or features that supported their decision. It is plausible that participants may have highlighted features that were not as important to reach this number, or more than 5 features were needed to support the decision. Additionally, the instruction to focus solely on attack type features may diminish the weight of more subtle textures or a combination of domain features and attack type features that eye tracking more naturally captures.

Finally, we report on the performance of the DINOv2 foundation models. Unlike past experiments that showed superior closed-set performance, the performance of DINOv2 models is mixed. In Table 1, only DINOv2 + SVM-RBF was able to exceed the XENT baseline while the other two variants, SVM-Linear and LogReg, failed to surpass the baseline performance. Furthermore, while SVM-RBF shows solid improvement in ”artificial”, ”synthetic”, and ”post-mortem” attack types, SVM-Linear and LogReg performance is explained by a large improvement in ”artificial” and equivalent or worse than baseline performance in all other categories. In Table 2, we see that all three methods

were near equivalent or worse than the XENT baseline with all three methods performing very well on "post-mortem" samples and generally poorly on all other attack types.

4.5. Limitations

We acknowledge some limitations of this work, which we address in this section. DINOv2 was tested due to its rising popularity and impressive capabilities in the iris PAD domain. However, we cannot guarantee open-set testing for any foundational model, including DINOv2, as we do not know which iris images, if any, were absorbed into the model training. In terms of performance, our results show that collectively eye tracking saliency maps outperformed hand annotations head-to-head while improving the D-NetPAD cross entropy baseline. Since collecting human saliency is expensive and time consuming, we set out to investigate if one type is better than the other for saliency-guided training. While our results show that eye tracking is the better candidate in open-set iris PAD, we acknowledge that further exploration in other domains is needed to validate a broader claim. Likewise, our results indicate that de-noising eye tracking maps led to an increase in performance. However, the dataset from Dowling *et al.* [17] was provided in two phases and only the Initial Eye Tracking maps experienced a performance bump from the de-noising while the performance of the De-noised Full ET maps largely stayed the same. Future studies should explore de-noising other eye tracking datasets and consider different clustering parameters depending on the task at hand.

5. Conclusion

This paper proposes VISER, a methodology for open-set iris PAD detection leveraging different methods and forms of saliency, including two distinct human saliency forms, for saliency-guided training. In our study, we compared the performance of these methods in AUROC and APCER at BPCER 1% against a D-NetPAD cross entropy baseline and reported on the improvement, or absence of, on this baseline. Our findings indicate that the best performing variant was De-noised Initial ET heatmaps with an average AUROC improvement of **0.0608** and an APCER at BPCER 1% improvement of **0.1063** over D-NetPAD indicating there is a noticeable performance improvement from de-noising eye tracking maps prior to saliency-guided training. The remaining eye tracking methods also showed noticeable improvements over D-NetPAD in both metrics whereas the majority of the other methods failed to make an impact. Neither the hand annotations, nor the segmentation masks, were able to improve over D-NetPAD in APCER at BPCER 1% and only the Equal Entropy hand annotations were able to marginally improve AUROC. Finally, we evaluated DINOv2 with three different classification methods inspired by prior work in closed set evaluations. Our results show

that while DINOv2 + SVM-RBF showed an AUROC improvement of **0.0485**, the other two methods, LogReg and SVM-Linear, failed to improve the baseline AUROC. In APCER at BPCER 1%, only LogReg made a marginal improvement over D-NetPAD while SVM-Linear and SVM-RBF failed to improve. We reported in our observations and limitations that we cannot truly guarantee open-set testing for DINOv2 models since we do not know its training data but that its performance increases largely occur on one attack type. Finally we discuss some limitations and discussed ways for future researchers to adapt this work. To facilitate follow up research efforts, the source codes, model weights, and saliency maps are offered along with this paper.

References

- [1] University of Notre Dame Open Source Iris Recognition Repository. <https://github.com/CVRL/OpenSourceIrisRecognition/>. Accessed: 12-14-25. 4
- [2] Chinese Academy of Sciences Institute of Automation (CASIA) Datasets Webpage. Accessed: 03-12-2021. 3
- [3] Warsaw University of Technology Datasets Webpage. <http://zbum.ia.pw.edu.pl/EN/node/46>, 2013. 3
- [4] Aidan Boyd, Zhaoyuan Fang, Adam Czajka, and Kevin W Bowyer. Iris presentation attack detection: Where are we now? *Pattern Recognition Letters*, 138: 483–489, 2020. 2
- [5] Aidan Boyd, Kevin W. Bowyer, and Adam Czajka. Human-aided saliency maps improve generalization of deep learning. In *Proceedings of the IEEE/CVF Winter Conference on Applications of Computer Vision (WACV)*, pages 2735–2744, 2022. 4
- [6] Aidan Boyd, Jeremy Speth, Lucas Parzianello, Kevin W Bowyer, and Adam Czajka. Comprehensive study in open-set iris presentation attack detection. *IEEE Transactions on Information Forensics and Security*, 18:3238–3250, 2023. 2, 7
- [7] Aidan Boyd, Patrick Tinsley, Kevin W Bowyer, and Adam Czajka. Cyborg: Blending human saliency into the loss improves deep learning-based synthetic face detection. In *Proceedings of the IEEE/CVF Winter Conference on Applications of Computer Vision*, pages 6108–6117, 2023. 2, 3
- [8] Ricardo JGB Campello, Davoud Moulavi, and Jörg Sander. Density-based clustering based on hierarchical density estimates. In *Pacific-Asia conference on knowledge discovery and data mining*, pages 160–172. Springer, 2013. 4
- [9] Corinna Cortes and Vladimir Vapnik. Support-vector networks. *Machine learning*, 20(3):273–297, 1995. 5

- [10] David R Cox. The regression analysis of binary sequences. *Journal of the Royal Statistical Society Series B: Statistical Methodology*, 20(2):215–232, 1958. 5
- [11] Colton R Crum and Adam Czajka. Mentor: Human perception-guided pretraining for increased generalization. In *2025 IEEE/CVF Winter Conference on Applications of Computer Vision (WACV)*, pages 7470–7479. IEEE, 2025. 2
- [12] Colton R Crum, Aidan Boyd, Kevin Bowyer, and Adam Czajka. Teaching ai to teach: Leveraging limited human saliency data into unlimited saliency-based training. *arXiv preprint arXiv:2306.05527*, 2023. 2
- [13] Adam Czajka and Kevin W Bowyer. Presentation attack detection for iris recognition: An assessment of the state-of-the-art. *ACM Computing Surveys (CSUR)*, 51(4):1–35, 2018. 2
- [14] Hao Dang, Feng Liu, Joel Stehouwer, Xiaoming Liu, and Anil K Jain. On the detection of digital face manipulation. In *Proceedings of the IEEE/CVF Conference on Computer Vision and Pattern Recognition*, pages 5781–5790, 2020. 2
- [15] Abhishek Das, Harsh Agrawal, Larry Zitnick, Devi Parikh, and Dhruv Batra. Human attention in visual question answering: Do humans and deep networks look at the same regions? *Computer Vision and Image Understanding*, 163:90–100, 2017. 3
- [16] John Daugman. How iris recognition works. In *The essential guide to image processing*, pages 715–739. Elsevier, 2009. 2
- [17] Byron Dowling, Jozef Porubcin, and Adam Czajka. Autosight: Automatic eye tracking-based system for immediate grading of human expertise. In *2025 IEEE Symposium on Visual Languages and Human-Centric Computing (VL/HCC)*, pages 355–366, 2025. 3, 8
- [18] Sukru Eraslan, Yeliz Yesilada, and Simon Harper. “the best of both worlds!” integration of web page and eye tracking data driven approaches for automatic aoi detection. *ACM Transactions on the Web (TWEB)*, 14(1):1–31, 2020. 4
- [19] Martin Ester, Hans-Peter Kriegel, Jörg Sander, Xiaowei Xu, et al. A density-based algorithm for discovering clusters in large spatial databases with noise. In *kdd*, pages 226–231, 1996. 4
- [20] Javier Galbally, Jaime Ortiz-Lopez, Julian Fierrez, and Javier Ortega-Garcia. Iris liveness detection based on quality related features. In *2012 5th IAPR International Conference on Biometrics (ICB)*, pages 271–276. IEEE, 2012. 3
- [21] Samuel Grieggs, Bingyu Shen, Greta Rauch, Pei Li, Jiaqi Ma, David Chiang, Brian Price, and Walter J Scheirer. Measuring human perception to improve handwritten document transcription. *IEEE Transactions on Pattern Analysis and Machine Intelligence*, 44(10):6594–6601, 2021. 2
- [22] Abhinav Hasija and Terry L Esper. In artificial intelligence (ai) we trust: A qualitative investigation of ai technology acceptance. *Journal of Business Logistics*, 43(3):388–412, 2022. 2
- [23] Sen He, Hamed R Tavakoli, Ali Borji, and Nicolas Pugeault. Human attention in image captioning: Dataset and analysis. In *Proceedings of the IEEE/CVF International Conference on Computer Vision*, pages 8529–8538, 2019. 2
- [24] John M Henderson. Human gaze control during real-world scene perception. *Trends in cognitive sciences*, 7(11):498–504, 2003. 3
- [25] Gao Huang, Zhuang Liu, Laurens Van Der Maaten, and Kilian Q Weinberger. Densely connected convolutional networks. In *Proceedings of the IEEE conference on computer vision and pattern recognition*, pages 4700–4708, 2017. 3
- [26] Jeff Huang, Ryen White, and Georg Buscher. User see, user point: gaze and cursor alignment in web search. In *Proceedings of the sigchi conference on human factors in computing systems*, pages 1341–1350, 2012. 3
- [27] Yupan Huang, Zhaoyang Zeng, and Yutong Lu. Be specific, be clear: Bridging machine and human captions by scene-guided transformer. In *Proceedings of the 2021 Workshop on Multi-Modal Pre-Training for Multimedia Understanding*, pages 4–13, 2021. 2
- [28] ISO/IEC 30107-3:2017. Information technology — biometric presentation attack detection — part 3: Testing and reporting. International standard, International Organization for Standardization, 2017. 3
- [29] Ming Jiang, Shaohuang Huang, Jibin Duan, and Qi Zhao. Salicon: Saliency in context. In *Proceedings of the IEEE Conference on Computer Vision and Pattern Recognition (CVPR)*, pages 1072–1080, 2015. 3
- [30] Marcel A Just and Patricia A Carpenter. A theory of reading: From eye fixations to comprehension. *Psychological review*, 87(4):329, 1980. 3
- [31] Tero Karras, Samuli Laine, Miika Aittala, Janne Hellsten, Jaakko Lehtinen, and Timo Aila. Analyzing and improving the image quality of stylegan. In *Proceedings of the IEEE/CVF conference on computer vision and pattern recognition*, pages 8110–8119, 2020. 2
- [32] Tero Karras, Miika Aittala, Samuli Laine, Erik Härkönen, Janne Hellsten, Jaakko Lehtinen, and Timo Aila. Alias-free generative adversarial networks. *Advances in neural information processing systems*, 34: 852–863, 2021. 2
- [33] Davinder Kaur, Suleyman Uslu, Kaley J Rittichier, and Arjan Durrezi. Trustworthy artificial intelligence:

- a review. *ACM computing surveys (CSUR)*, 55(2):1–38, 2022. 2
- [34] Naman Kohli, Daksha Yadav, Mayank Vatsa, and Richa Singh. Revisiting iris recognition with color cosmetic contact lenses. In *2013 International Conference on Biometrics (ICB)*, pages 1–7. IEEE, 2013. 3
- [35] Naman Kohli, Daksha Yadav, Mayank Vatsa, Richa Singh, and Afzel Noore. Detecting medley of iris spoofing attacks using DESIST. In *2016 IEEE 8th International Conference on Biometrics Theory, Applications and Systems (BTAS)*, pages 1–6. IEEE, 2016. 3
- [36] Sung Joo Lee, Kang Ryoung Park, Youn Joo Lee, Kwanghyuk Bae, and Jaihie Kim. Multifeature-based fake iris detection method. *Optical Engineering*, 46(12):127204–127204, 2007. 3
- [37] Bo Li, Peng Qi, Bo Liu, Shuai Di, Jingen Liu, Jiquan Pei, Jinfeng Yi, and Bowen Zhou. Trustworthy ai: From principles to practices. *ACM Computing Surveys*, 55(9):1–46, 2023. 2
- [38] Drew Linsley, Dan Shiebler, Sven Eberhardt, and Thomas Serre. Learning what and where to attend with humans in the loop. In *International Conference on Learning Representations*, 2019. 2
- [39] Susana Martinez-Conde, Stephen L Macknik, and David H Hubel. The role of fixational eye movements in visual perception. *Nature reviews neuroscience*, 5(3):229–240, 2004. 4
- [40] Daniel Moreira, Mateusz Trokielewicz, Adam Czajka, Kevin Bowyer, and Patrick Flynn. Performance of humans in iris recognition: The impact of iris condition and annotation-driven verification. In *2019 IEEE Winter Conference on Applications of Computer Vision (WACV)*, pages 941–949. IEEE, 2019. 2
- [41] Kien Nguyen, Hugo Proença, and Fernando Alonso-Fernandez. Deep learning for iris recognition: A survey. *ACM Comput. Surv.*, 56(9), 2024. 2
- [42] Maxime Oquab, Timothée Darcet, Théo Moutakanni, Huy Vo, Marc Szafraniec, Vasil Khalidov, Pierre Fernandez, Daniel Haziza, Francisco Massa, Alaaeldin El-Nouby, et al. Dinov2: Learning robust visual features without supervision. *arXiv preprint arXiv:2304.07193*, 2023. 3, 5
- [43] Alice J O’Toole, Xaiobo An, Joseph Dunlop, Vaidehi Natu, and P Jonathon Phillips. Comparing face recognition algorithms to humans on challenging tasks. *ACM Transactions on Applied Perception (TAP)*, 9(4): 1–13, 2012. 2
- [44] PayEye. Payeye: Biometric payment and identification solutions. <https://pay-eye.com/>, 2025. Accessed: 2026-02-09. 2
- [45] Jacob C Piland, Adam Czajka, and Christopher Sweet. Model focus improves performance of deep learning-based synthetic face detectors. *IEEE Access*, 11: 63430–63441, 2023. 2, 4
- [46] Floyd Ratliff and Lorrin A Riggs. Involuntary motions of the eye during monocular fixation. *Journal of experimental psychology*, 40(6):687, 1950. 4
- [47] Brandon Richard Webster, So Yon Kwon, Christopher Clarizio, Samuel E Anthony, and Walter J Scheirer. Visual psychophysics for making face recognition algorithms more explainable. In *Proceedings of the European Conference on Computer Vision (ECCV)*, pages 252–270, 2018. 2
- [48] Ioannis Rigas and Oleg V Komogortsev. Eye movement-driven defense against iris print-attacks. *Pattern Recognition Letters*, 68:316–326, 2015. 3
- [49] Bernhard Schölkopf, Alex J Smola, Robert C Williamson, and Peter L Bartlett. New support vector algorithms. *Neural computation*, 12(5):1207–1245, 2000. 5
- [50] Renu Sharma and Arun Ross. D-netpad: An explainable and interpretable iris presentation attack detector. In *2020 IEEE international joint conference on biometrics (IJCB)*, pages 1–10. IEEE, 2020. 3
- [51] Redwan Sony, Parisa Farmanifard, Hamzeh Alzwayry, Nitish Shukla, and Arun Ross. Benchmarking foundation models for zero-shot biometric tasks. *arXiv preprint arXiv:2505.24214*, 2025. 2, 5
- [52] Juan E. Tapia, Lázaro Janier González-Soler, and Christoph Busch. Towards iris presentation attack detection with foundation models. In *2025 IEEE 19th International Conference on Automatic Face and Gesture Recognition (FG)*, pages 1–5, 2025. 2, 5
- [53] Hamed R Tavakoli, Ahmed Pishe, Esa Rahtu, and Janne Heikkilä. Saliency revisited: Analysis of mouse movements versus fixations. In *Proceedings of the IEEE Conference on Computer Vision and Pattern Recognition (CVPR)*, pages 6354–6362, 2017. 3
- [54] Clare Teng, Harshita Sharma, Lior Drukker, Aris T Papageorghiou, and J Alison Noble. Visualising spatio-temporal gaze characteristics for exploratory data analysis in clinical fetal ultrasound scans. In *2022 Symposium on Eye Tracking Research and Applications*, pages 1–6, 2022. 4
- [55] Patrick Tinsley, Sandip Purnapatra, Mahsa Mitcheff, Aidan Boyd, Colton Crum, Kevin Bowyer, Patrick Flynn, Stephanie Schuckers, Adam Czajka, Meiling Fang, et al. Iris liveness detection competition (livdet-iris)—the 2023 edition. In *2023 IEEE International Joint Conference on Biometrics (IJCB)*, pages 1–10. IEEE, 2023. 2
- [56] Mateusz Trokielewicz, Adam Czajka, and Piotr Maciejewicz. Assessment of iris recognition reliability

- for eyes affected by ocular pathologies. In *2015 IEEE 7th International Conference on Biometrics Theory, Applications and Systems (BTAS)*, pages 1–6. IEEE, 2015. [3](#)
- [57] Mateusz Trokielewicz, Adam Czajka, and Piotr Maciejewicz. Assessment of iris recognition reliability for eyes affected by ocular pathologies. In *2015 IEEE 7th International Conference on Biometrics Theory, Applications and Systems (BTAS)*, pages 1–6. IEEE, 2015. [3](#)
- [58] Mateusz Trokielewicz, Adam Czajka, and Piotr Maciejewicz. Presentation attack detection for cadaver iris. In *2018 IEEE 9th international conference on biometrics theory, applications and systems (BTAS)*, pages 1–10. IEEE, 2018. [2](#)
- [59] Mateusz Trokielewicz, Adam Czajka, and Piotr Maciejewicz. Perception of image features in post-mortem iris recognition: Humans vs machines. In *2019 IEEE 10th International Conference on Biometrics Theory, Applications and Systems (BTAS)*, pages 1–8. IEEE, 2019. [2](#)
- [60] Mateusz Trokielewicz, Adam Czajka, and Piotr Maciejewicz. Post-mortem iris recognition with deep-learning-based image segmentation. *Image and Vision Computing*, 94:103866, 2020. [3](#)
- [61] Zhuoshi Wei, Tieniu Tan, and Zhenan Sun. Synthesis of large realistic iris databases using patch-based sampling. In *2008 19th International Conference on Pattern Recognition*, pages 1–4. IEEE, 2008. [3](#)
- [62] David Yambay, Benedict Becker, Naman Kohli, Daksha Yadav, Adam Czajka, Kevin W. Bowyer, Stephanie Schuckers, Richa Singh, Mayank Vatsa, Afzel Noore, Diego Gragnaniello, Carlo Sansone, Luisa Verdoliva, Lingxiao He, Yiwei Ru, Haiqing Li, Nianfeng Liu, Zhenan Sun, and Tieniu Tan. LivDet-Iris 2017 – Iris Liveness Detection Competition 2017. In *2017 IEEE International Joint Conference on Biometrics (IJCB)*, pages 733–741, 2017. [3](#)
- [63] David Yambay, Brian Walczak, Stephanie Schuckers, and Adam Czajka. LivDet-Iris 2015 – Iris Liveness Detection Competition 2015. In *2017 IEEE International Conference on Identity, Security and Behavior Analysis (ISBA)*, pages 1–6, 2017. [3](#)
- [64] Ruohan Zhang, Akanksha Saran, Bo Liu, Yifeng Zhu, Sihang Guo, Scott Niekum, Dana Ballard, and Mary Hayhoe. Human gaze assisted artificial intelligence: A review. In *IJCAI: Proceedings of the Conference*, page 4951. NIH Public Access, 2020. [2](#)
- [65] Tian Zhang, Hui Zhang, Xiuying Wu, Hang Zou, Dexin Zhang, and Jing Liu. Cross-device iris presentation attack detection based on image-text multimodal alignment. In *Proceedings of the 2024 2nd Asia Symposium on Image and Graphics*, page 199–206,

New York, NY, USA, 2025. Association for Computing Machinery. [2](#)